THE JOURNAL OF BIOLOGICAL CHEMISTRY
Vol. 274, No. 13, Issue of March 26, pp. 8561–8569, 1999

Printed in U.S.A.

Oxidation Regulates the Inflammatory Properties of the Murine S100 Protein S100A8*

(Received for publication, September 10, 1998, and in revised form, December 28, 1998)

Craig A. Harrison‡, Mark J. Raftery‡, John Walsh‡, Paul Alewood§, Siiri E. Iismaa‡¶, Soula Thliveris‡, and Carolyn L. Geczy‡‖

From the ‡Cytokine Research Unit, School of Pathology, The University of New South Wales, Kensington, New South Wales 2052 and the §Centre for Drug Design and Development, The University of Queensland, St. Lucia, Queensland 4072, Australia

The myeloid cell-derived calcium-binding murine protein, S100A8, is secreted to act as a chemotactic factor at picomolar concentrations, stimulating recruitment of myeloid cells to inflammatory sites. S100A8 may be exposed to oxygen metabolites, particularly hypochlorite, the major oxidant generated by activated neutrophils at inflammatory sites. Here we show that hypochlorite oxidizes the single Cys residue (Cys^{41}) of S100A8. Electrospray mass spectrometry and SDS-polyacrylamide gel electrophoresis analysis indicated that low concentrations of hypochlorite (40 μM) converted 70–80% of S100A8 to the disulfide-linked homodimer. The mass was 20,707 Da, 92 Da more than expected, indicating additional oxidation of susceptible amino acids (possibly methionine). Phorbol 12-myristate 13-acetate activation of differentiated HL-60 granulocytic cells generated an oxidative burst that was sufficient to efficiently oxidize exogenous S100A8 within 10 min, and results implicate involvement of the myeloperoxidase system. Moreover, disulfide-linked dimer was identified in lung lavage fluid of mice with endotoxin-induced pulmonary injury. S100A8 dimer was inactive in chemotaxis and failed to recruit leukocytes *in vivo*. Positive chemotactic activity of recombinant Ala^{41}S100A8 indicated that Cys^{41} was not essential for function and suggested that covalent dimerization may structurally modify accessibility of the chemotactic hinge domain. Disulfide-dependent dimerization may be a physiologically significant regulatory mechanism controlling S100A8-provoked leukocyte recruitment.

Murine S100A8, also known as CP-10 (chemotactic protein, 10 kDa), myeloid-related protein 8, and calgranulin A (1), is a small acidic protein containing two Ca^{2+}-binding EF hands belonging to the highly conserved S100 protein family (2). Most S100 proteins appear to function as intracellular calcium-modulated proteins that may regulate diverse functions including cell growth, differentiation, energy metabolism, cytoskeletal-membrane interactions, and kinase activities (1, 3). Extracellular activities have been ascribed to at least five family members, and since our description of the chemotactic activity of S100A8, similar functions for S100A2 (S100L, chemotactic for guinea pig eosinophils) and S100A7 (psoriasin, chemotactic for human $CD4^+$ T lymphocytes and neutrophils) have been reported (4, 5). S100B is an extracellular neurotrophic factor, and mitogen (6) and human S100A8 and S100A9 are antimicrobial and cytostatic (7) and have been associated with inflammatory pathologies (reviewed in Ref. 8).

S100A8 is constitutively expressed with S100A9 in neutrophils. It is up-regulated by bacterial lipopolysaccharide (LPS)[1] and interleukin 1 in macrophages (9) and microvascular endothelial cells (10) and has been associated with neutrophil recruitment in abscess formation (11) and bleomycin lung (12). Our recent experiments also indicate an important role for S100A8 in embryogenesis where it is expressed by migrating trophoblasts, and deletion of the gene was lethal at mid-gestation.[2] We recently demonstrated S100A8 secretion from LPS-activated murine macrophages (9), and in the absence of a secretion signal sequence, Rammes *et al.* (13) proposed a novel tubulin-dependent pathway for S100A8/A9 release from activated human monocytes which may provide a paradigm for the secretion of other S100 proteins.

S100A8 was isolated as a soluble product of activated murine spleen cells (14) and in the picomolar range stimulates myeloid cell chemotaxis *in vitro* (15) and a sustained leukocyte recruitment, with mononuclear cell infiltration following an early influx of neutrophils, *in vivo* (15, 16). Together with TGF-β, it is one of the most potent chemotactic factors described. In contrast to the classical chemoattractants such as fMet-Leu-Phe, C5a, and the chemokines, S100A8 and TGF-β affect cytoskeletal actin polymerization and cell migration without causing degranulation and activation (17).

ApoS100 proteins form antiparallel, noncovalently linked dimers in solution (18, 19), and at physiological concentrations in reducing environments, S100B would most likely exist as a non-covalent homodimer (20). In contrast, the extracellular neurotrophic and mitogenic activities of S100B are dependent on redox status and inter- or intrachain disulfide bond formation (6, 21). Although there is no structural information, disulfide-mediated dimerization may also regulate some extracellular functions of other S100 proteins (19).

* This work was supported in part by grants from the National Health and Medical Research Council of Australia. The costs of publication of this article were defrayed in part by the payment of page charges. This article must therefore be hereby marked "*advertisement*" in accordance with 18 U.S.C. Section 1734 solely to indicate this fact.

¶ Present address: Victor Chang Cardiac Research Institute, Sydney, New South Wales 2010, Australia.

‖ To whom correspondence should be addressed: Cytokine Research Unit, School of Pathology, The University of New South Wales, Kensington, New South Wales 2052, Australia. Tel.: 61-2-9385-1599; Fax: 61-2-9385-1389.

[1] The abbreviations used are: LPS, lipopolysaccharide; TGF, transforming growth factor; C5a, complement factor 5; Me_2SO, dimethyl sulfoxide; PMA, phorbol 12-myristate 13-acetate; EAMS, endotoxin-activated mouse serum; OCl^-, hypochlorite; DTT, dithiothreitol; PAGE, polyacrylamide gel electrophoresis; ESI-MS, electrospray ionization-mass spectra; HBSS, Hanks' balanced salt solution; RP-HPLC, reverse phase-high pressure liquid chromatography; PMN, polymorphonuclear; PBS, phosphate-buffered saline; NEM, *N*-ethylmaleimide; dHL-60, differentiated HL-60.

[2] R. J. Passey, E. Williams, C. Wells, A. M. Lichanska, C. L. Geczy, S. Hu, M. H. Little, and D. A. Hume, submitted for publication.

Noncovalent heteromeric complexes of human S100A8 and S100A9 (also known as myeloid-related protein 14 and calgranulin B (1)) have been characterized (22) and are thought to represent the functional form, even though these proteins are not always coordinately expressed (23). Our recent experiments confirm the propensity of murine S100A8 to form non-covalent dimers in solution, and this property is independent of calcium and covalent disulfide bond formation (24). Murine S100A8 comprises 88 amino acids with a single cysteine residue at position 41 (14). Here we show that the monomeric (non-covalent dimeric) form of S100A8 was functional, whereas the oxidized homodimer was chemotactically inactive. S100A8 was readily oxidized by hypochlorite, a myeloperoxidase product generated by activated neutrophils and macrophages and implicated in the pathogenesis of inflammation and atherogenesis (25, 26). The efficiency by which stimulated neutrophils oxidized exogenous S100A8 suggests that the redox status of Cys^{41} of S100A8 may represent a physiologically relevant regulatory mechanism controlling S100A8-provoked leukocyte recruitment *in vivo*.

EXPERIMENTAL PROCEDURES

Materials

RPMI 1640 and fetal bovine serum were purchased from Life Technologies, Inc. Hanks' balanced salt solution (HBSS), HBSS (without $CaCl_2$ and $MgCl_2$), bovine serum albumin, sodium hypochlorite, dimethyl sulfoxide (Me_2SO), phorbol 12-myristate 13-acetate (PMA), *N*-ethylmaleimide (NEM), and Triton X-100 were purchased from Sigma. T4 DNA ligase, restriction enzymes, and Complete protease inhibitors were obtained from Boehringer Mannheim (Mannheim, Germany), and thioglycollate was from Difco.

S100A8 Analogues

Preparation and isolation of recombinant (r)S100A8 is described in detail (27, 28). Synthetic S100A8 and the α-aminobutyric acid derivative (Aba^{41}S100A8) will be described elsewhere.[3] All S100A8 preparations were homogeneous by SDS-PAGE and ESI-MS analysis. Recombinant proteins differed from their synthetic and native counterparts by an additional dipeptide, Gly-Ser, at the N terminus (27), and these residues were designated as positions −2 and −1.

For Ala^{41}S100A8 the oligonucleotide-directed mutagenesis was performed using the double take double-stranded mutagenesis kit from Stratagene (La Jolla, CA). Briefly, plasmid pS100A8-9 containing a 286-base pair *Bam*HI fragment encoding the S100A8 cDNA (27) was linearized at the unique *Sca*I restriction enzyme site in the ampicillin resistance gene, biotinylated at the 3′ ends with terminal deoxynucleotidyl transferase, purified from free biotinylated nucleotide using avidin-coated beads, and separated into single strands by alkali denaturation. A *Sca*I extension primer complementary to the terminal 18 bases of the 3′ end of the template strand (5′-ACTCACCAGTCACAGAAA-3′) and the Ala mutagenic primer complementary to the same strand and containing base changes that alter codon specificity from Cys^{41} to Ala^{41} (5′ACAAACTGAGG*AGCC*TCAGT AGTGAC-3′) were annealed to the captured template strand and extended with T7 DNA polymerase and T4 DNA ligase. The strands were denatured using NaOH, and the mutant strand was collected in the supernatant. A *Sca*I bridging primer containing 18 bases complementary to the *Sca*I extension primer and 6 bases complementary to the first 6 bases on the other side of the *Sca*I site (5′-TTTCTGTGACTGGTGAGTACTCAA-3′) was annealed to the mutant strand thereby recircularizing the strand and extended with T7 DNA polymerase and T4 DNA ligase. The double-stranded closed circular molecules incorporating the mutation in both strands were transformed into XL-1 Blue *Escherichia coli* (Stratagene). The sequence of the mutated cDNA insert of one such recombinant, designated pS100A8-9.1, was verified by the chain termination method of DNA sequencing prior to subcloning into the *Bam*HI site of the Glutagene pGEX2T bacterial expression vector (AMRAD Pharmacia Biotech, Melbourne, Australia) to produce the recombinant expression plasmid $pAla^{41}$S100A8.

High Performance Liquid Chromatography (HPLC)

All liquid chromatographic separations were performed using a nonmetallic LC 625 HPLC system and UV absorbance monitored at 214 and 280 nm with a Waters 490 UV/visible detector. Samples were analyzed by C4 RP-HPLC using a Vydac 300 Å, 5 μm, 250 × 4.6 mm, C4 reverse phase column and gradient of 25–70% acetonitrile (0.1% trifluoroacetic acid) at 1 ml/min over 30 min. Fractions with major $A_{214\ nm}$ were collected manually.

Mass Spectrometry

Electrospray ionization (ESI)-mass spectra were acquired using a single quadrupole mass spectrometer equipped with an electrospray ionization source (Platform, VG-Fisons Instruments, Manchester, UK). Samples (~50 pmol, 10 μl) were injected into a moving solvent (10 μl/min; 50:50 water:acetonitrile, 0.05% trifluoroacetic acid) using a Phoenix 40 HPLC pump (VG-Fisons Instruments) coupled directly to the ionization source via a fused silica capillary (50 μm × 40 cm). The source temperature was 50 °C, and nitrogen was used as the nebulizer and drying gas. Sample droplets were ionized at a positive potential of approximately 3 kV and transferred to the mass analyzer with a cone voltage (sample cone to skimmer lens voltage) of 50 V. The peak width at half-height was 1 Da. Spectra were acquired in multi-channel acquisition mode over the mass range 700 to 1800 Da in 5 s and then calibrated with horse heart myoglobin (Sigma). Some spectra were recorded using a HP LC/MSD 1100 mass spectrometer (Hewlett-Packard, Palo Alto, CA) using similar conditions.

Oxidation of S100A8

Hypochlorite Oxidation—Recombinant S100A8, Ala^{41}S100A8, S100A9, hS100A8 (purified from human PMN)[4] and bovine S100B (Sigma) were used. Generally, 100 μg of S100 protein was reconstituted with 1 ml of PBS, pH 7.5 (final concentration 10^{-5} M). Hypochlorite, from a stock solution of 45 mM (determined as described previously (40)) was diluted in PBS, pH 7.5, to working solutions of 200 μM to 20 mM. S100 proteins were treated with increasing concentrations of hypochlorite (10–100 μM) for 15 min on ice before an equal volume of 2 × SDS-PAGE sample mixture (±100 mM DTT) was added, and samples were heated (100 °C, 3 min) and analyzed by 10% SDS-PAGE and silver staining or Western blotting using anti-S100A8. Alternatively, after 15 min, samples were fractionated by RP-HPLC and the eluted peaks analyzed by mass spectrometry.

Copper Oxidation—Recombinant S100A8 (100 μl of 1 mg/ml) purified from C4 RP-HPLC (29) was reduced in volume by two-thirds (Speedvac; Savant, Farmingdale, NY). An equal volume of ammonium bicarbonate (0.1 M) was added prior to the addition of copper sulfate (50 mM) to a final concentration of 2 mM. After 30 min at room temperature S100A8 homodimer was separated from residual monomer by C4 RP-HPLC.

PMA-induced Oxidation of S100A8 by Myeloid Cells—The human promyelocytic cell line, HL-60, was differentiated to the granulocytic lineage with Me_2SO (1.25%) for 5 days as described (30). dHL-60 cells were washed twice in HBSS or Ca^{2+}-free HBSS and resuspended (10^7 cells/ml) in the same solutions. Alternatively, murine PMN (10^7 cells/ml) elicited 6 h after intraperitoneal injection of thioglycollate as described (31) were used. Recombinant S100A8 (final concentration 10^{-5} or 5×10^{-7} M) was added to cell suspensions (10^6 cells) that were subsequently activated with PMA (1 μg/ml) and incubated for 20 min at 37 °C. The rate of PMA-induced oxidation of S100A8 was measured by incubating dHL-60 cells with PMA (1 μg/ml) for 1–30 min. After incubation, an equal volume of 2× SDS-PAGE sample mixture was added, and samples were analyzed by 10% non-reducing SDS-PAGE and silver staining or Western blot analysis using anti-S100A8. In some experiments sodium azide (10 nM to 100 μM) was included. All results shown are representative of at least three experiments.

Induction of LPS-induced Pulmonary Injury

Male Quakenbush Swiss mice, aged 8 weeks, were from the Animal Breeding and Holding Unit, University of New South Wales and experimental procedures complied with the requirements of the University's Animal Care and Ethics Committee (reference number 96/124).

Lipopolysaccharide (LPS; Difco, *E. coli* 055:B5), 10 μg/60 μl, was placed on the nares and introduced into the lung by inhalation according to the method of Szarka *et al.* (52). Control mice received 60 μl of PBS, pH 7.2. Each group comprised four mice. Animals were killed by exsanguination after an overdose of pentobarbital at 48 h after intranasal instillation. The lungs were perfused with 0.9% saline under a pressure of 40 cm of H_2O for 60 s to remove blood from the capillary bed. The trachea was then cannulated with a blunted 19-gauge needle and lungs lavaged. Bronchoalveolar lavage fluid was obtained by washing

[3] P. Alewood, manuscript in preparation.

[4] M. J. Raftery and C. L. Geczy, submitted for publication.

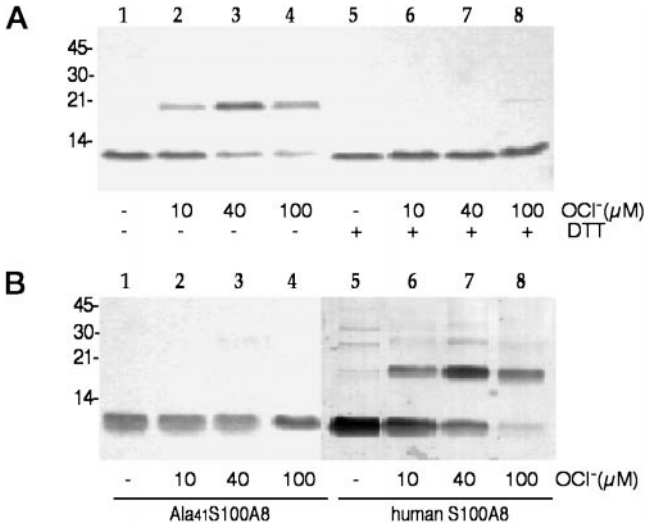

FIG. 1. **Hypochlorite oxidizes S100A8 to the covalent dimer.** *A*, recombinant murine S100A8 (10 μM) was either untreated (*lanes 1* and *5*) or treated with increasing concentrations of hypochlorite. Proteins were separated on SDS-PAGE in the absence (*lanes 1–4*) or presence (*lanes 5–8*) of 100 mM DTT prior to silver staining. *B*, Ala^{41}S100A8 (10 μM, *lanes 1–4*) or human S100A8 (10 μM, *lanes 5–8*) were treated identically to murine S100A8 and proteins separated on SDS-PAGE in the absence of reducing agents. Relative positions of molecular mass markers, in kDa, are shown in both gels.

the lungs three times repeatedly with 1 ml of PBS containing 10 mM *N*-ethylmaleimide (NEM). NEM was included to prevent artifactual formation of disulfide-linked S100A8 during isolation. Cells were pelleted (4 °C, 1200 rpm, 10 min), and in agreement with earlier studies (52), this procedure yielded 150–250-fold increases in neutrophil numbers after 48 h. Supernatants were processed by SDS-PAGE and Western blot analysis.

Chemotaxis Assay

S100A8 analogues (10 μg) lyophilized (Speedvac) with glycerol (5 μl) were stored at −80 °C. Reconstitution was with 10 μl of 0.1% trifluoroacetic acid and 990 μl RPMI 1640 to give a 10^{-6} M stock solution that was serially diluted in RPMI 1640, 0.1% bovine serum albumin immediately before use. The murine monocytoid cell line WEHI 265 was used as responding cell (27), and chemotaxis was performed in a 48-well microchemotaxis Boyden chamber (Neuro Probe Inc., Bethesda, MD) as described (15). Endotoxin-activated mouse serum (EAMS, 5%) was used as a positive control. Coomassie Blue/crystal violet was used to stain the membranes and migrating cells quantitated (10× objective) using planimetry measurements obtained from image analysis (Wild-Leitz, Lane Cove, Australia). Data were analyzed using the Student's *t* test (* $p < 0.01$ *versus* controls).

Leukocyte Recruitment in Vivo

S100A8 analogues (30 μg) were reconstituted in 10 μl of 0.1% trifluoroacetic acid, neutralized to pH 6.5 with 0.1 M sodium phosphate, and made to 1 ml with phenol red-free HBSS (PRF-HBSS) containing 0.1% ovalbumin (5× crystalline, Calbiochem). S100A8 solutions were held overnight at 4 °C and subsequently diluted with 2 ml of PRF-HBSS, 0.1% ovalbumin (S100A8 final concentration 10^{-6} M). Specific pathogen-free female Balb/c mice (6–8 weeks) were injected intraperitoneally with 1 ml of S100A8 (final concentration 10 μg per mouse), or analogues, or vehicle control solution, sacrificed after 16 h (maximal leukocyte recruitment occurred between 16 and 24 h (32)), and cells harvested by peritoneal lavage with 5 ml HBSS, 0.38% citrate, washed twice, and counted.

RESULTS

Hypochlorite Oxidation of S100 Proteins—Hypochlorite (OCl^-) is a major oxidant produced by neutrophils in an inflammatory response (25), and the susceptibility of recombinant murine S100A8 (10 μM) to oxidation by hypochlorite was tested. Fig. 1*A* shows SDS-PAGE separation of rS100A8 samples treated with increasing concentrations of OCl^- (*lanes 2–4*). In contrast to the untreated monomeric form (*lane 1*), which migrated with an apparent M_r of 10,000, as little as 10 μM OCl^- converted approximately 20% of the S100A8 monomer to a higher molecular weight species (*lane 2*), and this increased to 70–80% with 40 μM OCl^- (*lane 3*). The higher molecular weight band (M_r 20,000) reacted with anti-S100A8 IgG in Western blot analysis and corresponded to disulfide-bonded S100A8 dimer (data not shown). No obvious higher molecular weight complexes were evident in any of the samples (*lanes 2–4*). At higher OCl^- concentrations (100 μM, *lane 4*) there was an apparent loss of protein detected by silver staining. Hypochlorite-induced dimerization of S100A8 occurred consistently in 10 separate experiments. Reduction of OCl^--oxidized samples with 100 mM DTT prior to electrophoresis resolved mainly components of M_r 10,000 (Fig. 1*A*, *lanes 6–8*) with a minor amount of the 20-kDa species remaining in the sample treated with the highest concentration of OCl^- (*lane 8*), indicating the formation of a disulfide bond in the OCl^--induced S100A8 dimer. The resistance of Ala^{41}S100A8 (a mutated form in which Ala^{41} was substituted for Cys^{41}) to OCl^--mediated dimerization (Fig. 1*B*, *lanes 1–4*), even at high OCl^- concentrations (100 μM, *lane 4*), confirmed the formation of disulfide-linked dimers in the native form. The native human S100A8 responded to OCl^- in a similar manner (Fig. 1*B, lanes 5–8*). Higher molecular weight components were apparent in oxidized (Fig. 1*B, lanes 6–8*) and non-oxidized (Fig. 1*B, lane 5*) samples, and these represent minor contaminants in the native preparation as levels did not change with OCl^- treatment.

Murine S100A9 forms a non-covalent heterodimer with S100A8 (34) and contains a free Cys residue at position 110 (29). In contrast to S100A8, OCl^- treatment of murine S100A9 failed to form covalent dimers of the expected mass (~28 kDa). Instead, stepwise increases in apparent molecular weight were evident with increasing concentrations of OCl^- (up to ~1 kDa at 40 μM and ~2 kDa at 250 μM, Fig. 2*A*). Silver staining indicated no apparent loss of S100A9 when OCl^- concentrations >100 μM were used (Fig. 2*A*, *lane 5*).

When low amounts of OCl^- were added to equimolar mixtures of S100A8 and S100A9 (Fig. 2*B*) only low levels (<5%) of the disulfide-linked heterodimer (24 kDa) were formed. Silver staining indicated that S100A8 was predominantly oxidized to the 20-kDa homodimer and oxidation was almost complete with 40 μM OCl^-. In contrast, S100A9 was principally converted to a higher molecular weight (~16 kDa), monomeric form (see Fig. 2*A*, *lane 5*). Western blot analysis with anti-S100A8 confirmed preferential formation of disulfide-linked S100A8 homodimer after oxidation with OCl^- (Fig. 2*C*). Anti-S100A8 also reacted with the heterodimer even though this represented <5% of the reaction product (Fig. 2*B*). Anti-S100A9 recognized the oxidized monomeric forms of S100A9 (Fig. 2*D, lanes 2–4*) and reacted well with the low levels of heterodimer (24 kDa) and homodimer (28 kDa) generated after oxidation with OCl^-.

Characterization of OCl^--oxidized S100A8—The concentration of OCl^- required to convert murine S100A8 monomer (retention time 19.2 min by C4 RP-HPLC) to predominantly dimer was specific. With 10 μM S100A8 and 10 μM OCl^- in the assay, a small amount of product with a retention time of 19.8 min was evident by HPLC analysis (Fig. 3*A*). SDS-PAGE analysis indicated that this species had an apparent M_r of 20,000 and reacted with anti-S100A8 IgG by Western blotting (not shown). Approximately 70–80% of S100A8 was converted to the higher molecular weight form by 40 μM OCl^- (Fig. 3*B*). Small amounts of apparently monomeric S100A8 (19.2 min) and other reaction products (18.4–19.0 min) were evident. Higher concentrations of OCl^- (100 μM) produced multiple oxidation species (Fig. 3*C*), and total protein recovery was

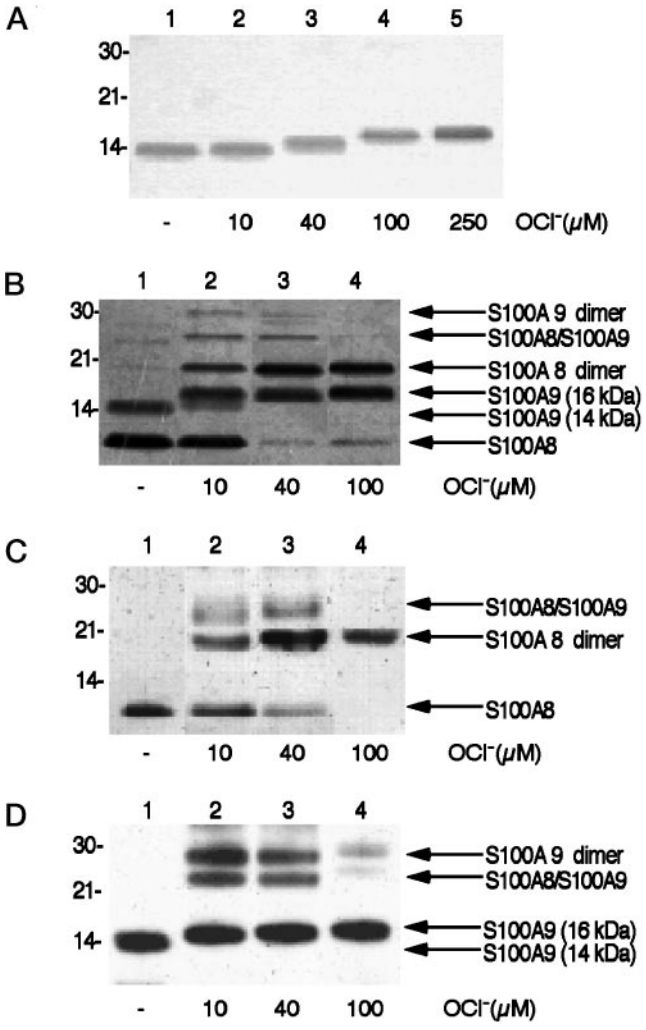

FIG. 2. **Murine S100A9 fails to form disulfide-linked homodimers following hypochlorite oxidation.** *A*, S100A9 (10 μM) was either untreated (*lane 1*) or treated with increasing concentrations of hypochlorite. Proteins were separated on SDS-PAGE in the absence of reducing agents prior to silver staining. *B*, equal concentrations of S100A8 and S100A9 (5 μM) were mixed and either untreated (*lane 1*) or treated with increasing concentrations of hypochlorite. Proteins were separated on SDS-PAGE in the absence of DTT. Molecular weight markers for both gels are shown. To better identify the molecular species in *B*, Western blot analyses using anti-S100A8 (*C*) and anti-S100A9 (*D*) antibodies were performed.

reduced by ~75%.

Table I compares the masses determined by ESI-MS of rS100A8 derivatives isolated after OCl^- (40 μM) treatment with those determined previously for S100A8 monomer (29). Hypochlorite oxidation generated both modified monomeric and dimeric species. The monomeric form (retention time 19.2 min., Fig. 3*B*) had an additional 46 Da associated with it, and the addition of three oxygens (mass 48 Da) may account for this increased mass. The main oxidation product (retention time 19.8 min, Fig. 3*B*) had a mass of 20,707 Da confirming that, at 40 μM OCl^-, disulfide bond formation was the most likely outcome. The additional 92 Da associated with this product presumably represents the dimeric form of the modified monomer. Characterization of these modifications are in progress.

A major aim of this study was to assess the activity of the murine S100A8 dimer *in vivo* and *in vitro*. Although OCl^- oxidation of S100A8 generated a dimeric species, RP-HPLC profiles and mass spectrometry data suggested that formation of a disulfide bond was not the only modification. Screening of other potential agents indicated that Cu^{2+} oxidized S100A8

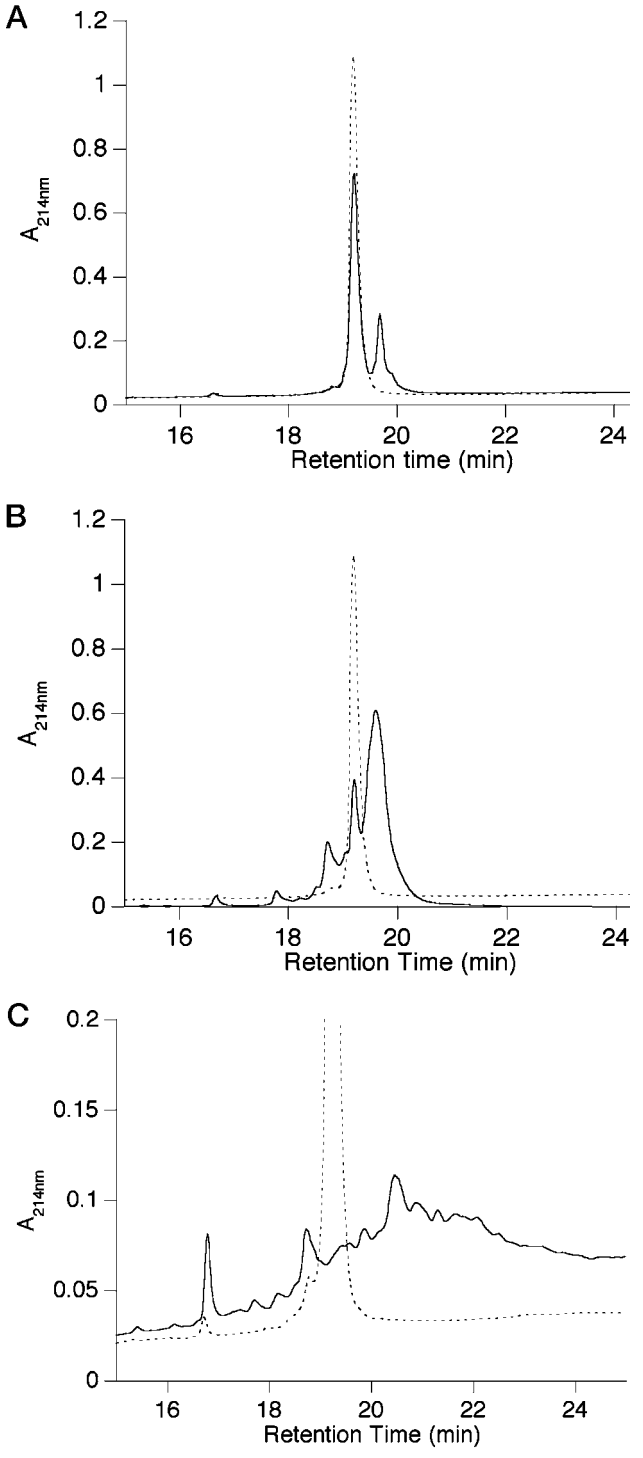

FIG. 3. **Comparison of C4 RP-HPLC elution profiles of S100A8 oxidized by hypochlorite.** rS100A8 (10 μM) was oxidized with 10 μM (*A*), 40 μM (*B*), and 100 μM (*C*) hypochlorite for 15 min and fractionated by C4 RP-HPLC. The elution profile of untreated rS100A8 from C4 RP-HPLC is shown by the *dashed line*.

more efficiently than OCl^- and produced a more homogeneous product. Fig. 4 shows that Cu^{2+} converted approximately 85% of S100A8 monomer to a single oxidative product with retention time of 19.80 min and mass of 20,615 ± 2 Da (*inset*). The mass was identical to the predicted mass (20,615 Da) of the disulfide-linked form, and reduction with DTT totally converted the dimer to monomer of mass 10,308 Da.

PMA-activated HL-60 Granulocytic Cells Oxidize S100A8—To determine whether murine S100A8 could be oxidized as a

TABLE I

ESI mass spectrometry of hypochlorite-treated rS100A8 derivatives

Untreated rS100A8 (10 μM) or that treated with 40 μM OCl^- (see Fig. 3B) were subjected to mass spectrometry as described. ND, not determined.

Sample	HPLC retention time	ESI mass	Provisional assignment
	min	*Da*	
rS100A8 OCl^- oxidation	19.3	10,307.5	
	18.7	ND	
	19.2	10,353	Modified rS100A8 with additional 46 Da
	19.8	20,707	Disulfide-linked dimer of modified rS100A8 (+92)

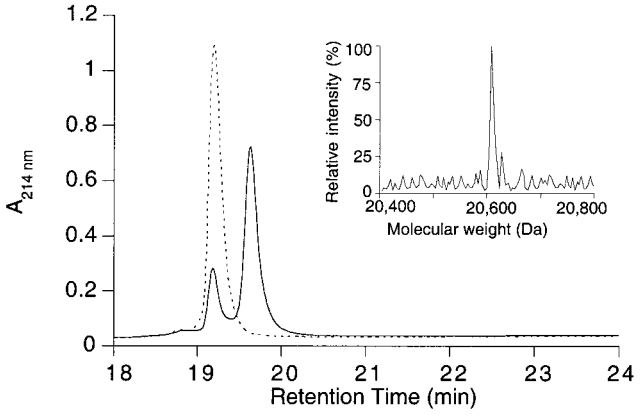

FIG. 4. **S100A8 is susceptible to copper oxidation.** Elution profile of rS100A8 (20 μg) from C4 RP-HPLC (*dashed line*) and after treatment with 2 mM $CuSO_4$ for 30 min is shown. S100A8 homodimer, elution time 19.8 min (*solid line*), was separated from residual monomer by RP-HPLC. *Inset,* ESI mass spectrum of copper-oxidized S100A8 homodimer.

consequence of neutrophil activation, differentiated (d)HL-60 granulocytic cells were activated with PMA using defined conditions that generate an oxidative burst by these cells (30). Generation of oxygen metabolites was confirmed by reduction of nitro blue tetrazolium in our experiments. Fig. 5*A* shows a time course of PMA-induced dHL-60 oxidation of exogenous S100A8 (10 μM). Unstimulated cells (*lane 1*) did not convert S100A8 to dimer over 30 min, whereas PMA (1 μg/ml) triggered the rapid oxidation of monomer to dimer, evident after 1 min (*lane 2*) and with 95% conversion within 10 min (*lane 6*). Using this concentration of PMA, no loss of S100A8 was evident during the time course. It is noteworthy that no additional major oxidation products were evident under these experimental conditions and that cell-induced dimers were reduced by DTT. Thioglycollate-elicited murine PMN oxidized S100A8 in the same manner in response to PMA activation (not shown).

Similarly, levels of S100A8 identified in inflammatory conditions such as rheumatoid plasma (~600 nM) (53) and cystic fibrosis plasma (~200 nM) (54), when added to PMA-activated dHL-60 cells, were also oxidized to the disulfide-linked homodimer. Western blot analysis shows that monomer (Fig. 5*B*, *lane 1*) to dimer (*lane 6*) conversion of 500 nM S100A8 occurred 30 min after neutrophil activation. Anti-S100A8 reacted somewhat more strongly with the homodimer than the monomer.

The susceptibility of S100A8 to OCl^--induced oxidation suggested the involvement of the myeloperoxidase-H_2O_2-halide system in the cellular oxidation of S100A8. This was supported by the inhibitory effects of the myeloperoxidase inhibitor sodium azide on S100A8 oxidation. Fig. 5*C* shows that PMA-activated dHL-60 cells, in the absence of sodium azide, converted all S100A8 to the dimer in 30 min (*lane 2*). At low azide concentrations (10–100 nM, *lanes 3* and *4*) no inhibition occurred, whereas higher concentrations reduced dimer formation (1–10 μM, *lanes 5* and *6*), and oxidation was abolished at azide concentrations exceeding 100 μM (*lanes 7* and *8*).

S100A8 Homodimer Formation at the Site of LPS-induced Pulmonary Injury—Bronchoalveolar lavage fluid obtained from mice after LPS inhalation contained significantly more neutrophils than from PBS-treated controls. Protein levels in the extracellular fluid were higher (Fig. 6, *lane 2*) in the treated group and components migrating at 10 and 20 kDa (*arrows*) were increased. Western blot analysis (Fig. 6, *lane 4*) confirmed S100A8 monomer and homodimer in LPS-induced fluid. No S100A8/A9 covalent complex was observed. A 70-kDa protein also reacted with anti-S100A8 and may represent a high molecular weight complex of S100A8. This component and the dimer were reduced by DTT (Fig. 6, *lane 5*) indicating disulfide bond formation.

Chemotactic Activity of S100A8 and Analogues—S100A8 and analogues were tested for their chemotactic activity *in vitro*. Fig. 7 shows that WEHI monocytoid cells had little spontaneous migration (45 ± 24 cells/field) but responded to increasing dilutions of rS100A8 in a characteristic bell-shaped profile (27), with optimal activity at 10^{-11} M (226 ± 32 cells/field). The recombinant mutant, Ala^{41}S100A8, was also active with a dose response similar to that of the unmodified recombinant protein (200 ± 34 cells/field) although potency at higher (>10^{-10} M) and lower (<10^{-12} M) concentrations was consistently less than that of the unmodified form. Checkerboard analysis, performed as described (15), confirmed chemotactic rather than chemokinetic activity for Ala^{41}S100A8. Table II compares the chemotactic activity of all available murine S100A8 analogues at their optimal chemotactic concentrations.

Native S100A8, synthetic, and Aba^{41}S100A8 all had optimal activities of 10^{-12} M and were of similar potencies. Aba^{41}S100A8 recruited somewhat greater numbers of cells, although differences between the preparations were not statistically significant. Furthermore, potencies of these analogues were similar to the positive control, 5% EAMS (contains C5a). In agreement with our earlier report demonstrating the chemotactic potential of rS100A8 (27), the optimal activities of rS100A8 and Ala^{41}S100A8 were some 10-fold less (10^{-11} M) than the native and synthetic forms, but similar numbers of cells were recruited. In marked contrast, Cu^{2+}-oxidized S100A8 homodimer recruited 66 ± 20 cells when tested at 10^{-11} and 72 ± 31 with 10^{-12} M, and although these values were consistently higher, recruitment was not significantly different ($p < 0.5$) from control values (45 ± 24 cells/field). No migration above control values was evident at other concentrations tested (Fig. 7). The OCl^--oxidized dimeric form of S100A8 also failed to recruit WEHI cells (not shown).

Leukocyte Recruitment in Vivo—Table III shows that intraperitoneal injection of the monomeric forms of S100A8, including the Cys to Ala/Aba mutants, stimulated leukocyte recruitment after 16 h. As described earlier for $S100A8^{42–55}$ (15), infiltrates consisted of mixtures of neutrophils and monocytes at this time. Although responses were variable between different batches of mice, they were greater than controls ($p < 0.01$), and no differences were obvious between preparations. In contrast, little leukocyte infiltration occurred in the buffer-injected controls (1.2 ± 0.5 × 10^6 cells) or in mice injected with disulfide-linked dimer (1.5 ± 0.8 × 10^6 cells) prepared by Cu^{2+} oxidation. Dose-response curves indicated that 5–10 μg of the

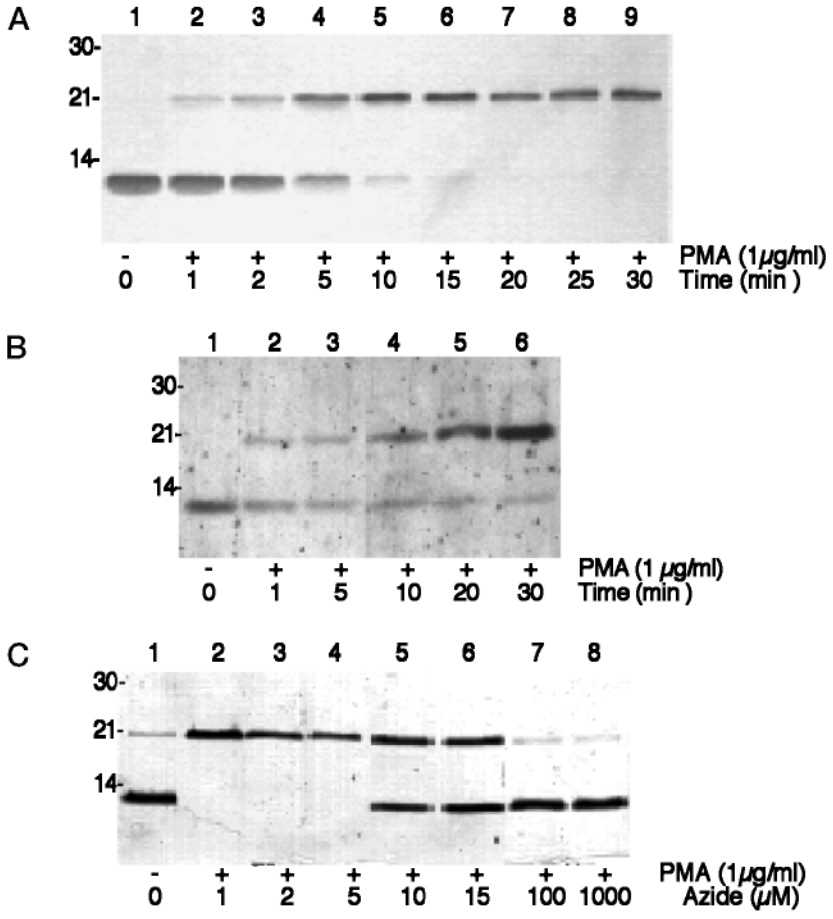

FIG. 5. **PMA-induced dHL-60 cellular oxidation of rS100A8.** *A*, time course of PMA-induced dHL-60 oxidation of S100A8. S100A8 (10 μM) was added to unstimulated (*lane 1*) or PMA-stimulated (1 μg/ml, *lanes 2–9*) dHL-60 cells, and the reaction was allowed to proceed for various times. Proteins were separated on SDS-PAGE in the absence of reducing agent and silver stained. *B*, at more physiological concentrations of S100A8, Western blot analysis was required to visualize protein. S100A8 (500 nM) was added to unstimulated (*lane 1*) or PMA-stimulated (1 μg/ml, *lanes 2–6*) dHL-60 cells, and samples were analyzed as described above. *C*, S100A8 (10 μM) was added to unstimulated (*lane 1*) or PMA-stimulated (1 μg/ml PMA, *lanes 2–8*) dHL-60 cells for 30 min at 37 °C in the absence (*lane 2*) or presence of increasing sodium azide concentrations. Following incubation samples were analyzed by 10% SDS-PAGE and silver staining. Relative positions of molecular weight markers are shown.

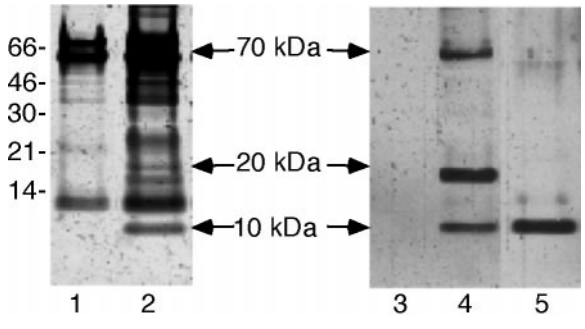

FIG. 6. **S100A8 dimer formation at the site of LPS-induced pulmonary injury.** Total protein present in BAL fluid of PBS control animals (*lane 1*) was compared with BAL fluid from LPS-treated animals (*lane 2*) by silver staining. The positions of 10- and 20-kDa proteins up-regulated in response to LPS are indicated (*arrows*). The same samples were analyzed by Western blotting using anti-S100A8 (PBS control, *lane 3*; LPS-treated, *lane 4*). The LPS-treated lung lavage sample was also reduced with 100 mM DTT (*lane 5*). The relative positions of molecular weight markers are shown.

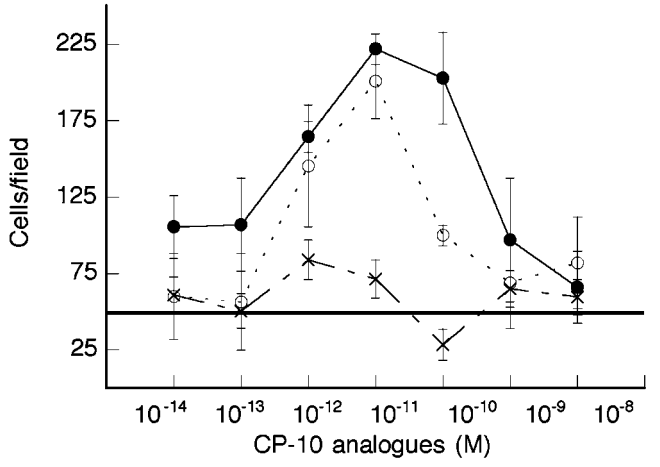

FIG. 7. **The covalent S100A8 homodimer is not chemotactic.** The chemotactic response of WEHI 265 cells toward rS100A8 (●), Ala^{41}S100A8 (○), and S100A8 homodimer (×). Migration in the absence of a chemotactic stimulus is given (*solid line*). Data represent the mean ± S.E. of results obtained from three separate experiments in which four to five grid fields of triplicate determinations were quantitated.

S100A8 analogues (5×10^{-7}-10^{-6} M) provoked optimal responses.

DISCUSSION

Intracellular S100 proteins exist mainly as non-covalent homo- or heterodimers with free reduced sulfhydryl groups. However, the demonstration that disulfide formation (whether inter- or intrachain) is required for the extracellular neurotrophic and mitogenic activities of S100B (6, 21) suggests that S100 proteins contain specific amino acids that are prone to oxidation, and that this reaction may selectively regulate bioactivity (35). In view of the sensitivity of cysteine residues to oxidation, and of their potentially important functional role in defining target protein-binding sites in S100 proteins (36, 37), our strategy was to determine whether oxidation of the single Cys residue at position 41 modified murine S100A8 function.

PMNs secrete granular enzymes and oxygen metabolites following exposure to activating agents such as PMA and to classical chemoattractants (38). The two-electron (non-radical) oxidant hypochlorite is a major product of stimulated neutrophils that produce superoxide radicals which dismute to H_2O_2 and are then converted into hypohalous acids by myeloperoxi-

TABLE II
Chemotactic responses provoked by S100A8 and analogues

The chemotactic potential of S100A8 and analogues were tested in chemotaxis assays using WEHI 265 as indicator cells. Data represent the mean ± S.E. of results obtained from three separate experiments in which cells migrated in five grid fields in triplicate determinations were quantitated. BSA, bovine serum albumin.

Chemoattractant	Cells/field
Control, RPMI 1640, 0.1% BSA	45 ± 24
nS100A8 (10^{-12}M)[a]	215 ± 52[b]
sS100A8 (10^{-12}M)	192 ± 53[b]
Aba_{41}S100A8 (10^{-12}M)	273 ± 84[b]
rS100A8 (10^{-11}M)	226 ± 32[b]
Ala_{41}S100A8 (10^{-11}M)	200 ± 34[b]
S100A8 homodimer (10^{-12}M)	72 ± 31
5% EAMS[c]	235 ± 77[b]

[a] The abbreviations used are: N, native; s, synthetic; Aba, α-aminobutyric acid; r, recombinant; Ala, recombinant mutant. The S100A8 homodimer was the covalent form prepared by copper oxidation and purified as shown in Fig. 4.
[b] $p < 0.01$ compared with controls.
[c] 5% endotoxin-activated mouse serum (EAMS) was used as positive control in all experiments.

TABLE III
Leukocyte recruitment in response to S100A8 analogues in vivo

S100A8 analogues (10 μg in 1 ml of HBSS, 0.1% ovalbumin) or diluent (control) were injected intraperitoneally into Balb/c mice as described under "Experimental Procedures." The leukocyte infiltrate was harvested by peritoneal lavage 16 h later, and total cells were quantitated. Data represent the mean ± S.E. of results obtained from four or five experiments in which a minimum of three mice/experiment were injected.

Chemoattractant	Cells recruited ($\times 10^6$)
Diluent control	1.2 ± 0.5
nS100A8	7.9 ± 4.5[a]
sS100A8	6.8 ± 1.4[a]
Aba_{41}S100A8	8.0 ± 5.0[a]
rS100A8	9.7 ± 4.7[a]
Ala_{43}S100A8	8.1 ± 3.4[a]
S100A8 homodimer	1.5 ± 0.8

[a] $p < 0.01$ compared to diluent control values.

dase in the presence of halides (25). Hypochlorite-modified proteins are implicated in inflammatory processes. For example, human α_1-proteinase inhibitor contains a critical methionine (position 358) in its reactive center, which is susceptible to OCl^- oxidation (39), rendering it an ineffective inhibitor of neutrophil elastase (39). Hypochlorite-oxidized proteins have also been identified in human atherosclerotic lesions (26), and OCl^- can transform lipoprotein into a high uptake form without significant lipid oxidation. ApoB-100, the single major protein associated with low density lipoprotein, is the main target for this oxidant (40) which becomes aggregated and cross-linked.

S100A8 and S100A9 are constitutive cytoplasmic proteins in neutrophils and are released in high concentrations at inflammatory sites (11, 12, 41) making them potential candidates for OCl^--mediated oxidation. Indeed, S100A8 oxidation to the disulfide-linked dimer increased from 20% in the presence of 10 μM hypochlorite to 70–80% with 40 μM hypochlorite (Fig. 1*A*). The physiological significance of this mechanism is highlighted by the observation that activated neutrophils (10^6) can generate as much as 124 μM hypochlorite within 2 h of stimulation (42). Covalent disulfide bond formation in response to OCl^- was confirmed by mass spectral analysis (Table I), by reduction of dimer to monomer with 100 mM DTT (Fig. 1*A*), and by the failure of Ala^{41}S100A8 to dimerize, even at high concentrations of oxidant (Fig. 1*B*). In keeping with its high structural similarity to the murine protein (14), the response of human S100A8 to OCl^- was similar (1*B*). Cys^{42} of human S100A8 and Cys^{41} of murine S100A8 are in the α-helix immediately preceding the hinge region (a 13-amino acid domain separating the two calcium-binding EF hand domains), and similar responses were not unexpected. Nitric oxide, another important product of activated myeloid cells, reacts readily with free radicals such as superoxide anion ($O_2^{\cdot-}$) to form peroxynitrite ($ONOO^-$), and NO and its oxidation products can modify thiols to yield biologically active reaction products (33). The NO donor SIN-1 and peroxynitrite anion oxidized S100A8 to the disulfide-linked dimer, but neither was as effective as OCl^- (not shown).

In contrast to S100A8, OCl^- failed to convert murine S100A9 into disulfide-linked homodimers (Fig. 2*A*) although it decreased its apparent electrophoretic mobility, possibly by oxidizing susceptible amino acids, including the Cys at position 110 and the 7 Met residues, resulting in changes in conformation or net charge. The propensity for S100A8 and S100A9 to form disulfide-linked dimers in solution has not been characterized. To examine this, equimolar mixtures of the proteins were treated with OCl^-, but no significant amounts of covalent heterodimer were detected (Fig. 2*B*). In support of these findings, a model of the putative human S100A8-S100A9 complex by Hunter and Chazin (43) predicted that the distance between Cys^{42} in S100A8 and Cys^3 in S100A9 would make disulfide bond formation in the heterodimer highly unlikely. Our results indicate that although the free Cys (Cys^{110}) of murine S100A9 occurs in the extended C-terminal domain, disulfide heterodimerization was similarly unlikely (Fig. 2*B*).

Relative peak areas (RP-HPLC) after oxidation with hypochlorite (40 μM; Fig. 3*B*) showed approximately 75% conversion of S100A8 monomer to homodimer. Mass spectrometry indicated a mass of 20,707 ± 2 Da (Table I), some 92 Da greater than the Cu^{2+}-oxidized dimer. Thus, even at OCl^- concentrations lower than those likely to occur in an inflammatory response, modifications of amino acids, in addition to that at Cys^{41}, are indicated. These probably include incorporation of oxygen atoms at Met^{36} and Met^{73}. Interestingly, the potent chemoattractants, fMet-Leu-Phe and human C5a are inactivated by the myeloperoxidase-halide system by conversion of methionine to the sulfoxide (44). The ability of stimulated neutrophils to chemically modify chemoattractants may be one means of limiting excess accumulation of leukocytes and terminating the progression of acute inflammation. We are currently investigating whether specific oxidation of Met residues in S100A8 affect chemotactic activity.

At higher OCl^- concentrations (>100 μM), oxidation of S100A8 was less specific. C4 RP-HPLC indicated a heterogeneous assortment of products (Fig. 3*C*), and SDS-PAGE analysis confirmed multiple monomeric and dimeric species suggesting a variety of modifications of susceptible amino acids. Moreover, the large reduction in recovered protein (~75%) suggested that precipitation and/or aggregation had occurred (Figs. 1*A* and 3*C*). Similarly, OCl^- aggregates and cross-links low density lipoprotein (40) and H_2O_2 oxidation of albumin at molar ratios >30:1 causes precipitation, presumably due to the formation of polymeric albumin derivatives, and precipitation is proportional to the amount of peroxide added (46).

The physiological relevance of oxidation of murine S100A8 by OCl^- was highlighted by the ability of PMA-activated neutrophils to totally convert exogenous S100A8 to the covalent dimer (Fig. 5*A*). The myeloperoxidase inhibitor sodium azide totally inhibited the cell-mediated oxidation of S100A8 (Fig. 5*B*). With the presumption that sodium azide is solely an inhibitor of myeloperoxidase, we conclude from these data that myeloperoxidase products are responsible for the majority of cell-mediated S100A8 oxidation (47). Oxidation by 10^6 activated dHL-60 cells was rapid, with approximately 90% conver-

sion of 1 μg of S100A8 to the dimer within 10 min (Fig. 4*A*). Similar results were obtained with elicited murine neutrophils activated in the same manner. No loss/aggregation of S100A8 was evident during the cellular activation process. Furthermore, disulfide-linked homodimer, but not heterodimer, was detected in bronchoalveolar lavage fluid of endotoxin-treated mice, confirming the limited heterodimer conversion observed in Fig. 2. A higher molecular weight form, possibly corresponding to components formed by aggregation (see Fig. 3), was also detected.

In marked contrast to the potent chemotactic activity of recombinant, synthetic, and native S100A8, disulfide-linked S100A8 homodimer was inactive *in vitro* (Fig. 7 and Table II). Moreover, these S100A8 preparations recruited between 4.8- (sS100A8) and 6.5-fold (rS100A8) more leukocytes than the disulfide-linked dimer following intraperitoneal injection (Table III), suggesting that availability of unmodified Cys^{41} might be functionally important. Site-directed mutagenesis studies of S100B indicated that Cys^{68} and Cys^{84} were essential for extracellular neurotrophic and mitogenic activities (52). However, the Cys mutant forms of S100A8, recombinant Ala^{41}S100A8 and synthetic Aba^{41}S100A8, recruited similar numbers of leukocytes to their unmodified recombinant or synthetic counterparts *in vitro* and *in vivo* (Table III and Fig. 7) indicating that Cys^{41} was not essential for recruitment. This extends our earlier studies demonstrating chemotactic activity of the hinge region peptide of S100A8 ($S100A8^{42–55}$), although the potency of the peptide was somewhat less than the full-length form (14). These experiments indicate alternate mechanisms for inactivation of S100A8 bioactivity whereby disulfide interactions involving Cys^{41} may sterically hinder and/or structurally alter exposure of the chemotactic hinge domain to restrict cellular target recognition.

Inactivation of the chemotactic activity of S100A8 by hypochlorite oxidation may provide a mechanism for limiting excess accumulation of leukocytes and terminating the progression of acute inflammation. Recruitment of neutrophils from the vascular lumen into the pulmonary airspace of LPS-treated mice begins within hours of intranasal instillation, and these cells accumulate in the airways within 24–48 h (52). Although time course experiments are warranted, Fig. 6 indicates that S100A8 was oxidized to the homodimer and higher aggregates *in vivo* at the time that the inflammatory response entered the resolution phase.

The efficiency of OCl^- oxidation of S100A8 may have additional implications. Approximately 20% of cytoplasmic protein of neutrophils is S100A8 (48), and necrotic neutrophils have the potential to release large amounts following an inflammatory stimulus (11, 12, 41). Activated monocytes (13) and macrophages (9) also release the protein. Even in the presence of equimolar amounts of S100A9, high concentrations of S100A8 may be a preferential target of oxygen metabolites (OCl^-, NO), thereby protecting other tissue proteins from excessive oxidative damage. This may represent an important function of human S100A8 which, unlike the murine protein, is not chemotactic (15). Murine S100A8 may therefore have pro- or anti-inflammatory activity, depending on its extracellular concentration and circumstance of release. This may be particularly relevant at sites of Gram-negative infection. In support of an anti-inflammatory role, recent experiments in our laboratory[5] have demonstrated glucocorticoid-mediated up-regulation of S100A8 mRNA and protein in macrophages stimulated with LPS. Glucocorticoids released via the neuroendocrine-immune network during stress have an immunomodulatory function during infection and tissue invasion (49). The apparently opposing activities of promoting and modulating inflammation are not unique to S100A8. Transforming growth factor β1 (TGF-β) is implicated in embryogenesis, development, and immune and inflammatory processes and shares this paradoxical behavior (50). S100A8 is also implicated in embryogenesis and development (51), and TGF-β is also chemotactic for myeloid cells at picomolar concentrations (17). The studies presented here provide a novel mechanism of regulation of the chemotactic activity of S100A8 by the myeloperoxidase system in neutrophils and suggest that release of this abundant protein by dying neutrophils at acute inflammatory sites may have a protective role.

Acknowledgments—We thank C. Cornish, T. Nilsson, and T. Tao for assistance in chemotaxis assays; S. Thomas and R. Stocker for discussions in the early stages of this work; members of the Biomedical Mass Spectrometry Unit (UNSW) for access to the HP MSD/1100; and R. Kumar for performing lung lavage.

[5] R. J. Passey, Z. Yang, T. Yen, K. Ku, S. Hu, and C. L. Geczy, manuscript in preparation.

REFERENCES

1. Schafer, B. W., and Heizmann, C. W. (1996) *Trends Biochem. Sci.* **21,** 134–140
2. Kligman, D., and Hilt, D. C. (1988) *Trends Biochem. Sci.* **13,** 437–443
3. Zimmer, D. B., Cornwall, E. H., Landar, A., and Song, W. (1995) *Brain Res. Bull.* **37,** 417–429
4. Komada, T., Araki, R., Nakatani, K., Yada, I., Naka, M., and Tanaka, T. (1996) *Biochem. Biophys. Res. Commun.* **220,** 871–874
5. Jinquan, T., Vorum, H., Larsen, C., Madsen, P., Eamussen, H., Gesser, B., Etzerodt, M., Honore, B., Celis, J., and Thestrup-Pederson, K. (1996) *J. Invest. Dermatol.* **107,** 5–10
6. Barger, S. W., Wolchok, S. R., and Van Eldik, L. (1992) *Biochim. Biophys. Acta* **1160,** 105–112
7. Sohnle, P., Collins-Lech, C., and Weissner, J. (1991) *J. Infect. Dis.* **163,** 187–192
8. Johne, B., Fagerhol, M. K., Lyberg, T., Prydz, H., Brandtzaeg, P., Naess-Andresen, C. F., and Dale, I. (1997) *Mol. Pathol.* **50,** 113–123
9. Hu, S. P., Harrison, C., Xu, K., Cornish, C. J., and Geczy, C. L. (1996) *Blood* **87,** 3919–3928
10. Yen, T., Harrison, C., Devery, J., Leong, S., Iismaa, S., Yoshimura, T., and Geczy, C. (1997) *Blood* **90,** 4812–4821
11. Kocher, M., Kenny, P. A., Farram, E., Abdul, M. K., Finlay, J. J., and Geczy, C. L. (1996) *Infect. Immun.* **64,** 1342–1350
12. Kumar, R. K., Harrison, C. A., Cornish, C. J., Kocher, M., and Geczy, C. L. (1998) *Pathology* **30,** 51–56
13. Rammes, A., Roth, J., Goebeler, M., Klempt, M., Hartmann, M., and Sorg, C. (1997) *J. Biol. Chem.* **272,** 9496–9502
14. Lackmann, M., Cornish, C. J., Simpson, R. J., Moritz, R. L., and Geczy, C. L. (1992) *J. Biol. Chem.* **267,** 7499–7504
15. Lackmann, M., Rajasekariah, P., Iismaa, S. E., Jones, G., Cornish, C. J., Hu, S., Simpson, R. J., Moritz, R. L., and Geczy, C. L. (1993) *J. Immunol.* **150,** 2981–2991
16. Devery, J. M., King, N. J., and Geczy, C. L. (1994) *J. Immunol.* **152,** 1888–1897
17. Cornish, C. J., Devery, J. M., Poronnik, P., Lackmann, M., Cook, D. I., and Geczy, C. L. (1996) *J. Cell. Physiol.* **166,** 427–437
18. Kilby, P. M., Van Eldik, L. J., and Roberts, G. (1996) *Structure* **4,** 1041–1052
19. Potts, B., Smith, J., Akke, M., Macke, T. J., Okazaki, K., Hidaka, H., Case, D. A., and Chazin, W. J. (1995) *Nat. Struct. Biol.* **2,** 790–796
20. Drohat, A. C., Nenortas, E., Beckett, D., and Weber, D. J. (1997) *Protein Sci.* **6,** 1577–1582
21. Scotto, C., Mely, Y., Oshima, H., Garin, J., Cochet, C., Chambaz, E., and Baudier, J. (1998) *J. Biol. Chem.* **273,** 3901–3908
22. Teigelkamp, S., Bhardwaj, R., Roth, J., Meinardus-Hager, G., Karas, M., Sorg, C. (1991) *J. Biol. Chem.* **266,** 13462–13467
23. Goebeler, M., Roth, J., Burwinkel, F., Vollmer, E., Bocker, W., and Sorg, C. (1994) *Transplantation* **58,** 355–361
24. Raftery, M. J., and Geczy, C. L. (1998) *J. Am. Soc. Mass Spectrom.* **9,** 533–539
25. Dean, R., Fu, S., Stocker, R., and Davies, M. (1997) *Biochem. J.* **324,** 1–18
26. Hazell, L. J., Arnold, L., Flowers, D., Waeg, G., Malle, E., and Stocker, R. (1996) *J. Clin. Invest.* **97,** 1535–1544
27. Iismaa, S. E., Hu, S., Kocher, M., Lackmann, M., Harrison, C. A., Thliveris, S., and Geczy, C. L. (1994) *DNA Cell Biol.* **13,** 183–192
28. Raftery, M. J., Harrison, C. A., and Geczy, C. L. (1997) *Rapid Commun. Mass Spectrom.* **11,** 405–409
29. Raftery, M. J., Harrison, C. A., Alewood, P., Jones, A., and Geczy, C. L. (1996) *Biochem. J.* **312,** 285–293
30. Yu, H., Suchard, S. J., Nairn, R., and Jove, R. (1995) *J. Biol. Chem.* **270,** 15719–15724
31. Ryan, J., and Geczy, C. L. (1988) *J. Immunol.* **141,** 2110–2117
32. Lau, W., Devery, J. M., and Geczy, C. L. (1995) *J. Clin. Invest.* **95,** 1957–1965
33. Mahoney, C. W., Pak, J. H., and Huang, K. P. (1996) *J. Biol. Chem.* **271,** 28798–28804
34. Goebeler, M., Roth, J., Henseleit, U., Sunderkotter, C., and Sorg, C. (1993) *J. Leukocyte Biol.* **53,** 11–18
35. Yao, Y., Jas, G., Kuczera, K., Williams, T., Schoneich, C., and Squier, T. (1996) *Biochemistry* **35,** 2767–2787
36. Baudier, J., and Cole, R. D. (1988) *J. Biol. Chem.* **263,** 5876–5883

37. Johnsson, N., and Weber, K. (1990) *J. Biol. Chem.* **265,** 14464–14468
38. Weiss, S. J. (1989) *N. Engl. J. Med.* **320,** 365–376
39. Ossana, P. J., Test, S. T., Matheson, N. R., Regiani, S., and Weiss, S. J. (1986) *J. Clin. Invest.* **77,** 1939–1951
40. Hazell, L. J., van den Berg, J., and Stocker, R. (1994) *Biochem. J.* **302,** 297–304
41. Brun, J. G., Jonsson, R., and Haga, H. J. (1994) *J. Rheumatol.* **21,** 733–738
42. Wu, S., Boyer, C., and Pizzo, S. (1997) *J. Biol. Chem.* **272,** 20627–20635
43. Hunter, M. J., and Chazin, W. J. (1998) *J. Biol. Chem.* **273,** 12427–12435
44. Clark, R. A. (1982) *J. Immunol.* **129,** 2725–2728
45. Domigan, N. M., Charlton, T. S., Duncan, M. W., Winterbourne, C. C., and Kettle, A. J. (1995) *J. Biol. Chem.* **270,** 16542–16548
46. Naskalski, J. W. (1994) *Ann. Biol. Clin.* **52,** 451–456
47. Hansson, M., Asea, A., Ersson, U., Hermodsson, S., and Hellstrand, K. (1996) *J. Immunol.* **156,** 42–47
48. Hessian, P. A., Edgeworth, J., and Hogg, N. (1993) *J. Leukocyte Biol.* **53,** 197–204
49. Wilckens, T. (1995) *Trends Pharmacol. Sci.* **16,** 193–197
50. McCartney-Francis, N., and Wahl, S. (1994) *J. Leukocyte Biol.* **55,** 401–409
51. Roth, J., Goebeler, M., and Sorg, C. (1993) *Biochem. Biophys. Res. Commun.* **191,** 565–570
52. Szarka, R. J., Wang, N., Gordon, L., Nation, P., and Smith, R. H. (1997) *J. Immunol. Methods* **202,** 49–57
53. Berntzen, H. B., Olmez, U., Fagerhol, M. K., and Munthe, E. (1991) *Scand. J. Rheumatol.* **20,** 74–82
54. Golden, B. E., Clohessy, P. A., Russell, G., and Fagerhol, M. K. (1996) *Arch. Dis. Child.* **74,** 136–139

Oxidation Regulates the Inflammatory Properties of the Murine S100 Protein S100A8

Craig A. Harrison, Mark J. Raftery, John Walsh, Paul Alewood, Siiri E. Iismaa, Soula Thliveris and Carolyn L. Geczy

J. Biol. Chem. 1999, 274:8561-8569.
doi: 10.1074/jbc.274.13.8561
